Journal of Applied Ecology

British Ecological Society

Journal of Applied Ecology 2010, **47**, 47–56 doi: 10.1111/j.1365-2664.2009.01745.x

Inferring spatial structure from time-series data: using multivariate state-space models to detect metapopulation structure of California sea lions in the Gulf of California, Mexico

Eric J. Ward[1]*, Haridas Chirakkal[2], Manuela González-Suárez[2]†, David Aurioles-Gamboa[4], Elizabeth E. Holmes[1] and Leah Gerber[2]

[1]*National Marine Fisheries Service, Northwest Fisheries Science, Center, 2725 Montlake Boulevard East, Seattle, WA 98112, USA;* [2]*Ecology, Evolution and Environmental Sciences, School of Life Sciences, Arizona State University, Tempe, AZ 85287, USA;* [3]*Laboratoire d'Ecologie et Evolution CNRS – UMR 7625 Université Pierre et Marie Curie 7 Quai St Bernard, 75005 Paris, France; and* [4]*CICIMAR-IPN, Avenida IPN s/n Col. Playa Palo de Santa Rita 23096, La Paz Baja, Baja California Sur, Mexico*

Summary

1. Understanding spatial structure and identifying subpopulations are critical for estimating population growth rates and extinction risk, and as such essential for effective conservation planning. However, movement and spatiotemporal environmental data are often unavailable, limiting our ability to directly define subpopulations and their level of asynchrony.

2. This study applies a recently developed statistical technique using time-series analysis of abundance data to identify subpopulations. The approach uses multivariate state-space models and Akaike's Information Criterion-based model selection to quantify the data support for different subpopulation numbers and configurations. This technique is applied to the population of California sea lions *Zalophus californianus* in the Gulf of California, Mexico, distributed across 13 breeding sites.

3. The abundance of California sea lions in the Gulf of California has declined over the last decade, though not all areas have been equally affected. In light of this variation, it is important to understand the population structure to ensure accurate viability assessments and effective management.

4. Our data support the hypothesis that the Gulf of California sea lion population has four subpopulations, each with 2–5 breeding sites. The dynamics between several adjacent subpopulations were correlated, suggesting that they experience similar environmental variation. For each subpopulation, we estimated long-term growth rates, as well as the environmental and observation variation.

5. For most of the subpopulations, our estimates of growth rates were considerably lower than those previously reported. In addition, we found considerable variability across subpopulations in their projected risk of severe decline over the next 50 years.

6. *Synthesis and applications*. We illustrate a new multivariate state-space modelling technique that uses time series of abundance to quantify the data support for different subpopulation configurations. Our analysis of the California sea lion population in the Gulf of California indicates that the population is spatially structured into four subpopulations, each exhibiting distinct risks of extinction. Based on our results, we recommend that conservation and management efforts in the Gulf of California focus on the two subpopulations with high probabilities of extinction within the next 50 years (Northern Midriff, Southern Midriff). Multivariate state-space models provide a practical approach to determine the spatial structure of virtually any species; they may be particularly useful for species of conservation concern for which data on dispersal and environmental drivers are likely to be scarce.

*Corresponding author. E-mail: eric.ward@noaa.gov

†Present address: Laboratoire d'Ecologie et Evolution CNRS – UMR 7625 Universite Pierre et Marie Curie 7 Quai St Bernard, 75005 Paris, France

Key-words: extinction risk, metapopulation, multivariate state-space, spatial structure, stochastic growth rate, *Zalophus californianus*

Introduction

A large body of research on the dynamics of metapopulations, a population that is structured into multiple subpopulations, has established that the level of fragmentation and synchrony within a metapopulation plays a major role in determining its viability (Levins 1970; Goodman 1987; Pulliam 1988; Gilpin & Hanski 1991; Tilman & Kareiva 1997; González-Suárez & Gerber 2008). This research has shown that effective management must not only identify subpopulations, but also evaluate which subpopulations are robust and independent – and thus might act as buffers against declines, and which are correlated together – and thus have a more limited ability to buffer the metapopulation as a whole. Unfortunately, identifying subpopulations is not trivial. Even when long-term survey data are available from multiple sites, determining which sites behave as asynchronous subpopulations is difficult because survey data are often corrupted by observation errors and these errors may create the illusion of asynchrony and independence.

In this paper, we show how a statistical analysis using multivariate state-space models can be used to quantify the data support for different subpopulation configurations in a metapopulation. We apply this approach to an analysis of the population structure of California sea lions *Zalophus californianus* in the Gulf of California, Mexico. State-space models include separate models for the population process and the observations of that process. The advantage of using state-space models is that the total variance in a time series of observations can be partitioned into observation and process variance (Holmes 2001; de Valpine & Hastings 2002; Lindley 2003; Dennis *et al.* 2006). The latter refers to the variance in population growth rates over time (as a result of stochastic environmental conditions) while the former refers to observation variability. Separating these two types of uncertainty is critical because partitioning reduces the bias in the process variance estimates – a requirement for unbiased forecasting and extinction risk estimation (Holmes *et al.* 2007).

California sea lions are found along the Pacific coast of North America from British Columbia to the Gulf of California (Peterson & Bartholomew 1967; Carretta *et al.* 2007), although breeding is limited to areas south of the Channel Islands (California). The species has been subdivided into several subpopulations based on analyses of genetic and ecological data, but the number, composition and locations of these subpopulations varies among studies, even those based on similar data. For example, independent analyses of genetic data have proposed between one and three subpopulations within the Gulf of California (Maldonado *et al.* 1995; González-Suárez *et al.* 2009; Schramm *et al.* 2009). Discrepancies in the number of subpopulations are partly explained by the use of different molecular markers, namely female-inherited mtDNA vs. biparentally inherited nuclear DNA, which have different patterns because of the observed sex bias in the dispersal in this species (González-Suárez *et al.* 2009). In addition, the location and number of sampled sites differed among these genetic studies, and in some cases were limited to a single site within the Gulf of California (Maldonado *et al.* 1995).

Alternative subpopulation configurations have been proposed based on analyses of multiple ecological and environmental covariates: diet diversity, isotope data, sea surface temperature and chlorophyll concentration (Szteren 2006). However, the composition of these subpopulations (in terms of which breeding sites belong to which subpopulation) differed depending on the type of covariate used (e.g. diet vs. diseases). The inconsistency of results among these diverse studies reflects our current lack of understanding about the actual population structure of California sea lions in the Gulf of California. Improving our knowledge of the population structure and connectivity is critical for conservation efforts because different subpopulation configurations result in distinct estimates of long-term viability (Gerber 2006; Gonzalez-Suarez *et al.* 2006). Although, as a whole, the numbers of California sea lions in the Gulf of California have declined by more than 20% in the last decade (Szteren, Aurioles & Gerber 2006), some breeding sites show increasing trends, making it difficult to determine the overall viability of California sea lions in the area.

Ideally, the determination of population structure should be based on movement data and data describing the environmental factors that cause correlation across sites. Movement patterns are normally determined with mark–release–recapture studies, but these studies are often implausible for a species of concern (Mech & Shannon 2002). For example, obtaining long-term movement data on California sea lions would require permanent marking of young animals using branding, which raises multiple legal and ethical concerns (McMahon, Bradshaw & Hays 2006a; McMahon *et al.* 2006b). Marking needs to be followed by a long-term resighting programme. In a long-lived species, this is often logistically and financially challenging and management actions often cannot be postponed for 5–15 years. The result is that detailed movement data for a species of conservation concern are rarely available. Spatial data on important environmental factors are also rarely available, both for logistical reasons and because the factors that cause variation in demographic parameters are often unknown. Multivariate time-series analysis provides a way to detect the spatial patterns of correlation and synchrony across different sites and reveal the subpopulations, if they exist (Hinrichsen & Holmes 2009). Multivariate time-series analysis requires only time-series count data from multiple sites and offers a novel approach to test hypotheses about various subpopulation configurations and estimate growth rates, as well

as process and observation variability (Hinrichsen & Holmes 2009).

In this paper, we evaluate six alternative hypotheses about the number and configuration of subpopulations in the Gulf of California using survey data (1979–2006) consisting of sea lion counts from 13 breeding sites in the area. The different hypotheses are based on different proposed drivers for population structure: genetics, disease, diet and environmental factors (see Materials and methods). Each hypothesis is converted into an appropriate multivariate state-space model, and the best model is chosen using model-selection criteria. The estimated model is then used for forecasting and to provide a risk assessment that takes population structure into account.

Materials and methods

DATA COLLECTION

We collected abundance data from 1979 to 2006 from all 13 California sea lion breeding sites (rookeries) in the Gulf of California (Fig. 1) although surveys were not possible for all years at each site (Fig. 2). The study sites include Rocas Consag (RC), San Jorge (SJ), Los Lobos (LL), Granito (GR), Los Machos (LM), Los Cantiles (LC), El Partido (EP), San Pedro Nolasco (SN), San Pedro Martir (SM), San Esteban (SE), Rasito (RA), Los Islotes (LI) and Farallon de San Ignacio (FI). Animals at each site were counted once during the sea lion reproductive season from June to August (Peterson & Bartholomew 1967). During this time, > 77% of animals are on land; adult males defend territories and adult females give birth and nurse their young (Bonnell & Ford 1987). In addition, > 84% of pups are born from the end of May to the end of June (Garcia-Aguilar & Aurioles-Gamboa 2003); thus, our survey periods included most of the individuals born during the year's reproductive season. The breeding sites were surveyed by circumnavigating each site in a small fibreglass boat with an outboard engine, at a distance ≤50 m from the shoreline (Aurioles-Gamboa & Zavala-Gonzalez 1994; Zavala-Gonzalez & Mellink 1997). Counts were conducted between 07.00 and 19.00 h each day by one trained observer. For more details see the description of methods in Wielgus *et al.* (2008).

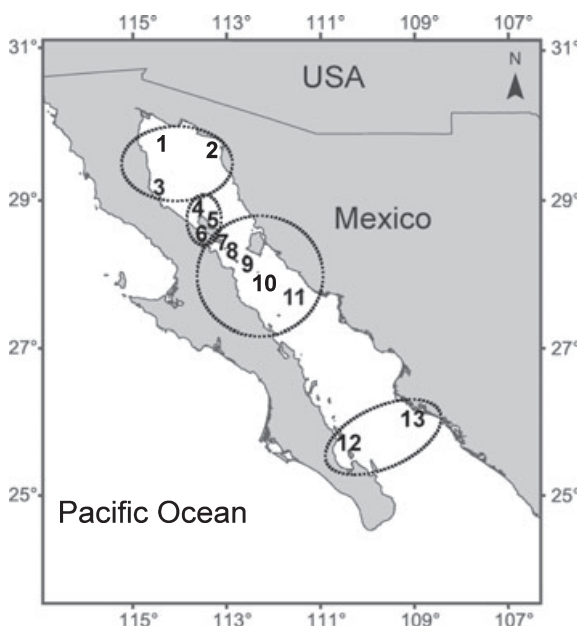

Fig. 1. Map of the Gulf of California, Mexico. The numbered sites correspond to: (1) Rocas Consag; (2) San Jorge; (3) Los Lobos; (4) Granito; (5) Los Cantiles; (6) Los Machos; (7) El Partido; (8) Rasito; (9) San Esteban; (10) San Pedro Martir; (11) San Pedro Nolasco; (12) Los Islotes; (13) Farallon de San Ignacio. Circles show the four subpopulations selected by the best-fit model (Table 1).

MULTIVARIATE AUTOREGRESSIVE STATE-SPACE MODEL

We used the multivariate state-space (MARSS) framework described by Hinrichsen & Holmes (2009) to model different population structures and to estimate population parameters, including process and observation variability. Process variability represents the temporal variability in population growth rate because of environmental stochasticity. This type of variation is multiplicative, as it appears in the growth rate term and becomes an additive term when the model is written as a function of log population size. Observation variation includes several types of error: sampling error resulting from only a portion of a population being sampled, measurement error resulting from inaccurate measurements (e.g. miscounting), and variability in sightability caused by a myriad of different environmental factors. In many ecological data sets, including the sea lion data analysed here, the sources of observation variation are confounded and cannot be independently estimated. Contrasted with process variation, observation variation has no bearing on current or future abundance, only our observations of that abundance.

State-space models have been applied to time series of ecological data because of their ability to separate out these two sources of variation, without the need of prior estimates of observation variance or replicated observations. The theory behind these models and their estimation is rooted in 50 years of maximum-likelihood (ML) research (reviewed in Harvey 1989; Shumway & Stoffer 2006; Roweis & Ghahramani 1999). State-space models are examining increasing application in ecology, both using ML (Holmes 2001; de Valpine & Hastings 2002; Shumway & Stoffer 2006) and Bayesian approaches (Meyer & Millar 1999; Clark & Bjørnstad 2004; Ward *et al.* 2007; Newman *et al.* 2009). The majority of the ecology literature has focused on the analysis of single time series (Staples, Taper & Dennis 2004; Dennis *et al.* 2006), however these methods have been extended to two-dimensional observations to analyse movement data (Jonsen, Myers & Flemming 2003). The MARSS framework used here (developed in Hinrichsen & Holmes 2009) is an extension of these established models to the multi-dimensional setting.

In the MARSS model, we use n to represent the number of discrete survey sites, and m to represent the number of unknown subpopulations. For the process model, $\mathbf{X}_t$ denotes the vector of length m representing true logarithmic subpopulation sizes in year t, $\mathbf{u}$ is an m-element vector of subpopulation growth rates, and $\boldsymbol{\eta}_t$ is a vector of length m representing the process errors in year t. We assume the process errors ($\boldsymbol{\eta}_t, \boldsymbol{\eta}_{t+1}, \ldots$) are serially uncorrelated in time, and drawn from a multivariate normal distribution with mean zero and variance-covariance matrix $\mathbf{Q}$. This assumption arises from stochastic properties of population processes (Dennis, Munholland & Scott 1991; Holmes *et al.* 2007). The multivariate population process in the MARSS model is given by

$$\mathbf{X}_{t+1} = \mathbf{X}_t + \mathbf{u} + \eta_t. \qquad \text{eqn 1}$$

When $\mathbf{Q}$ is a diagonal matrix, the trajectories of subpopulations are independent – we continue to describe this model as 'multivariate'

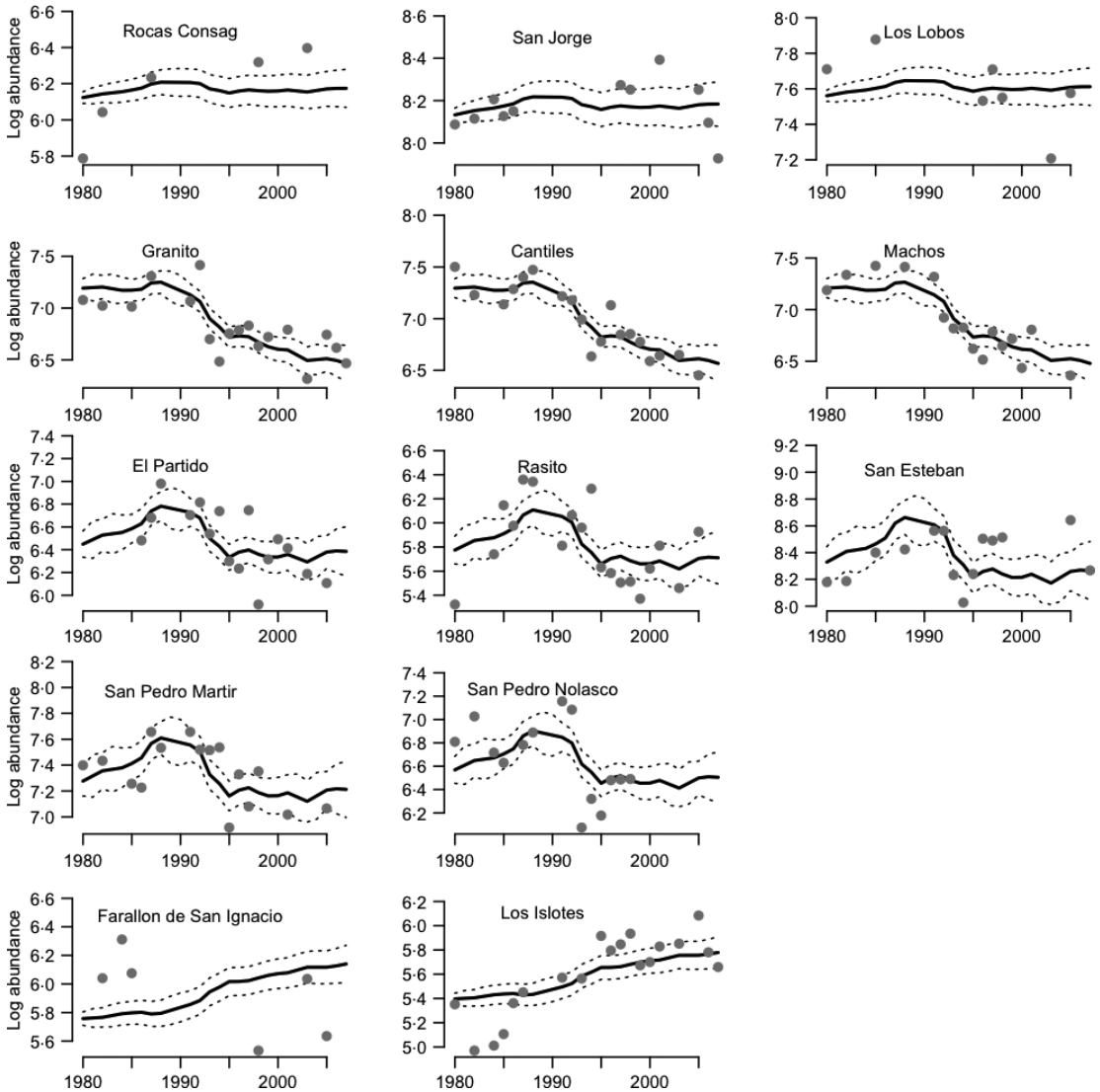

Fig. 2. Maximum-likelihood estimates (continuous line) of logarithmic subpopulation abundances and their 95% confidence intervals (CI) (dashed lines) for 13 sea lion breeding sites in the Gulf of California. Note that the CI are for the subpopulation trajectories not the observed data; thus that the data fall outside the CI is expected and simply depends on the site-specific observation errors. All estimates are derived from the best model with four correlated subpopulations (the distance model). Actual count data are shown by grey circles.

however, because multiple subpopulations are being modelled simultaneously. Divisions between subpopulations may be less discrete, and several subpopulations may have correlated dynamics (meaning good and bad years are correlated). We allow off-diagonal elements of **Q** to be non-zero in some of our models to incorporate this possibility.

The observation process in the MARSS model is given by

$$\mathbf{Y}_t = \mathbf{A} + \mathbf{Z}\mathbf{X}_t + \varepsilon_t, \qquad \text{eqn 2}$$

where $\mathbf{Y}_t$ is the n-element vector containing observed abundances at the n sites at time t. The number of sites (n) may be different from the number of subpopulations (m); **Z**, an $n \times m$ matrix of 0s and 1s, translates the m subpopulation sizes at time t into n observations at time t. When the number of sites is greater than the number of subpopulations, some sites are different observations of the same subpopulation trajectory. We use the n-element vector **A** to represent the mean bias between these sites. Observation errors are represented by the n-element vector $\boldsymbol{\varepsilon}_t$; like the process model, we assume that these errors are serially uncorrelated and distributed according to a multivariate normal distribution with a mean of 0 and variance-covariance matrix **R**. Equation 1 together with eqn 2 represent the complete MARSS model.

HYPOTHESES

Because of the flexibility of the MARSS approach, there are hundreds of thousands of combinations of models for this system. Our objective was not to find the model that fit the data best; rather our goal was to evaluate six different subpopulation configurations corresponding to the six hypotheses concerning the biological and environmental variables that determine the population structure. These hypotheses were based on previous work on the biology of sea lions in the Gulf of California and were developed independent of our analysis. For all hypotheses, $n = 13$, indicating 13 sites. These sites are all breeding sites (rookeries), but we refer to them simply as 'sites'. The hypotheses differ in terms of the number of subpopulations (m) and which sites belong to which subpopulation. The six hypotheses are:

• **Panmictic** ($m = 1$): all sites are part of a single large panmictic population. There is a single population trajectory, and all sites are independent observations of this trajectory.

• **DNA** ($m = 2$): sites are grouped into two subpopulations reflecting genetic stocks defined by mitochondrial and nuclear DNA variability (González-Suárez *et al.* 2009): Southern Baja Peninsula (LI, FI); and Upper Gulf of California (all other sites).

• **Diet** ($m = 4$): sites are grouped based on diet and environmental variables into four subpopulations (Szteren 2006): North (RC, SJ, LL); Northern Midriff (GR, LM, LC, EP); Southern Midriff (SN, SM, SE, RA); South (LI, FI). This configuration is similar to the one based on geographical distance (below), with the exception of the El Partido site.

• **Disease** ($m = 4$): sites are grouped into four subpopulations defined by shared pathogens (Szteren 2006): North (SJ, RC, LL, GR, LC, LM); North Central (EP, RA); Central (SE, SM, SN); South (FI, LI).

• **Distance** ($m = 4$): sites are grouped into four subpopulations defined by geographical distance: North (RC, SJ, LL); Northern Midriff (GR, LM, LC); Southern Midriff (SN, SM, SE, EP, RA); South (LI, FI). The geographical subpopulations were established using an agglomerative hierarchical cluster analysis (described in Gonzalez-Suarez *et al.* 2006) considering similarity based on distance from the RC rookery.

• **Independent** ($m = 11$): each site represents an independent subpopulation and thus each is an observation of an independent subpopulation trajectory.

Each hypothesis represents a basic structure: the number of subpopulations and which sites are within which subpopulation.

Within each of these six hypotheses, we tested different levels of complexity. We allowed the level of process variation (the year-to-year variability) to be different or equal across subpopulations and to be independent or correlated across subpopulations. Similarly, we allowed the growth rates to be different or equal across subpopulations. Although density dependence can be easily included in MARSS models (Dennis *et al.* 2006), we did not use models incorporating density dependence because California sea lion numbers have been declining in the Gulf of California as a whole (Fig. 2), and are thought to be below carrying capacity because of historical exploitation (Zavala-Gonzalez & Mellink 2000). As a diagnostic check, we reran our best-fit model using the density-dependent version of eqn 1 ($\mathbf{X}_{t+1} = \mathbf{B}\mathbf{X}_t + \mathbf{u} + \boldsymbol{\eta}_t$). The lowest diagonal element of the estimated **B** matrix was 0·9831, indicating virtually no support for density dependence (**B** = 1 represents density independent growth). For the observation model, we assumed that the observation errors were uncorrelated (diagonal **R** matrix). This assumption was required because of missing data (years with no census), however the assumption was reasonable given that observations were collected independently at each site. We tested models where the variance of the observation errors (the diagonal elements of **R**) was allowed to be different or forced to be equal across sites.

PARAMETER ESTIMATION, CONFIDENCE INTERVALS AND DIAGNOSTICS

We used the Kalman filter and EM algorithm (chapter 6, Shumway & Stoffer 2006) to obtain the ML parameters for each model. To ensure global maximization, we used 5000 independent runs initialized from different random starting points. To independently verify the parameter estimates, we compared the estimates with those using the data-cloning algorithm, an alternate ML algorithm for state-space models (Lele, Dennis & Lutscher 2007). Code for MARSS parameter estimation via the Kalman-EM and data-cloning algorithms are available at http://www.ecologybox.org/projects/kalman-em.

Approximate confidence intervals (CI) on MARSS parameters can be computed via numerical estimation of the Hessian matrix (Shumway & Stoffer 2006) or from the Markov chain Monte Carlo output from the data-cloning algorithm (Lele *et al.* 2007). These approximate CI are based on the large-sample properties of ML estimates. Because our sample size was relatively small (because of missing values), we used parametric bootstrapping (following Stoffer & Wall 1991) to estimate 95% CI. Five thousand data sets were simulated from the MARSS model using the ML parameter estimates and missing data inserted where it is present in the original data set. Parameters were then estimated for each of the bootstrapped data sets (as described above), and the 95-percentiles formed the parameter CI. Asymptotic confidence intervals for the estimated subpopulation sizes (Fig. 2) were generated from the standard errors output from the Kalman filter using the best-fit model (chapter 6, Shumway & Stoffer 2006).

MODEL SELECTION

Frequentist model selection is based on minimizing the difference (in terms of likelihood) of an estimated model relative to the distribution of possible data from a true (unknown) process (Burnham & Anderson 2002). Akaike's Information Criterion (AIC) is the most used estimator for this difference and is based on the ML of the model fit with a penalty term that measures the degree to which the complexity of the model leads to over-fitting (and thus an inflated likelihood value). The original AIC model-selection criterion is $\mathrm{AIC} = -2 \log L + 2K$, where the penalty term is the number of model parameters K. This is based on large-sample properties of the ML of a fitted model and is biased when the data set is small. A small-sample modification, $\mathrm{AIC}c = -2 \log L + 2K(K + 1)/(n - K - 1)$, is designed to correct this bias. However, for MARSS models, the small-sample problem is more extreme and AIC*c* severely underestimates the complexity penalty for this model class (Cavanaugh & Shumway 1997).

There are two versions of AIC that are designed specifically for state-space models. The first, AIC*b*, uses bootstrapping to estimate the penalty term (Cavanaugh & Shumway 1997); the second, AIC*i*, uses Monte Carlo simulation to estimate the penalty term (Bengtsson & Cavanaugh 2006). Because we were testing models with different **Z** matrices (in eqn 2), our model-selection option was constrained to AIC*b*. We followed Cavanaugh & Shumway's (1997) AIC*b* algorithm using a parametric bootstrap. The AIC*b* values were used to rank each model in terms of its data support, with lower AIC*b* indicating greater support. A model with an AIC*b* value that is eight points greater that from another model is considered weakly supported, relative to the competing model (Burnham & Anderson 2002). Our code for computation of AIC*b* model-selection criteria is available at http://www.ecologybox.org/projects/kalman-em.

FORECASTING

Metapopulation forecasting was performed by numerically simulating 1000 50-year subpopulation trajectories using eqn 1 with our best model (the distance model; Table 1) and the ML estimates of population growth rate (**u**) and the variance-covariance matrix (**Q**) for this model. Simulations were initialized from the estimated subpopulation sizes in 2006, and for each simulation, we calculated the probability

Table 1. Model performance, given by Akaike's Information Criterion (AIC) *b*-value, across the six hypotheses for the subpopulation configuration

Parameters			Hypotheses (m = no. subpopulations)					
u	**Q**	**R**	Panmictic (m = 1)	Diet (m = 4)	Disease (m = 4)	Distance (m = 4)	DNA (m = 2)	Independent (m = 11)
Same	Same	Same	68·2	48·4	49·8	26·8	38·9	22·2
Unique	Same	Same		63·9	72·8	46·9	46·6	25·5
Same	Unique	Same		55·8	57·6	26·6	34·2	64·4
Same	Same	Unique	97·3	74·4	73·2	68·4	67·3	32·5
Unique	Same	Unique		87·1	91·3	71·8	69·3	65·6
Unique	Unique	Same		61·4	84·1	39·8	38·3	50·0
Same	Unique	Unique		102·8	103·8	202·1	82·7	114·7
Unique	Unique	Unique		111·8	133·8	167·8	77·5	169·2
Same	Correlated	Same		40·3	63·1	37·0	38·3	4804·7
Unique	**Correlated**	**Same**		44·9	87·2	**13·7**	39·6	989·4
Same	Correlated	Unique		110·3	163·8	321·4	102·2	NA
Unique	Correlated	Unique		116·3	176·5	467·9	94·5	NA

Process errors (**Q**) may be independent (a diagonal matrix) with variances that are the same magnitude across subpopulations (same), independent with unequal variances across subpopulations (unique) or may be temporally correlated, meaning an unconstrained **Q** matrix (correlated). The growth rate (**u**) and observation error matrix (**R**) parameters may also be equal (same) or unique across subpopulations. The model best supported by the data is shown in bold; complex models that did not fully converge are not applicable.

of 20%, 50% and 80% declines in the four subpopulations over a 50-year forecast period. These forecasts assume that environmental variation over the next 50 years will be similar to that estimated during the study period. Only process variation (**Q**) was included in these projections because we are interested in the distribution of future true subpopulation sizes, rather than the distribution of observed survey counts.

Results

The best-supported model (lowest AIC*b*) is one with four subpopulations (Table 1), where the subpopulations are defined by geographical distances (Gonzalez-Suarez *et al.* 2006). No other models are supported (they have AIC*b*'s more than eight log-likelihood units higher than the best model). Under the geographical distances model (Fig. 1), the number of sites assigned to each subpopulation ranges from two (Southern) to five (Southern Midriff). This means that the group of sites within a subpopulation are sufficiently connected (presumably by movement) that their dynamics are synchronized. The best model allows each subpopulation to have a unique growth rate (Table 1). ML estimates of growth rates are negative for the Northern and Southern Midriff subpopulations, and positive for the North and South subpopulations (Table 1). However, the 95% CI for all subpopulations except the Southern subpopulation include 0. Our process variance estimates are low (σ^2 = 0·004–0·0005), but still within the range estimated for other large vertebrates (Holmes *et al.* 2007). Our observation variance is also low (σ^2 = 0·042) relative to other marine surveys, but it is also still within the range of other studies. Converting the observation variance in log-space to the covariance (CV) in normal space results in a CV of *c.* 0·21. In comparison, a recent study of 21 species of cetaceans from the US west coast showed CV ranging from 0·19 to 1·25 (Barlow & Forney 2007).

The best model has an unconstrained variance–covariance matrix **Q** for the process variation. This configuration allows each subpopulation to have a distinct process variance, but also allows correlation in the year-to-year variation between subpopulations (Table 2). The Southern subpopulation correlates negatively with the other three; when the South experiences favourable conditions, other subpopulations experience negative conditions. Meanwhile, the North Midriff and South Midriff populations appear to experience nearly identical envi-

Table 2. Maximum-likelihood estimates of subpopulation growth rates (**u**), process variances (**Q**) and correlation matrix of process variation between subpopulations for the best model (Table 1)

			Correlation (**Q**)			
Subpopulation	Growth rates (**u**)	Process σ^2 (**Q**)	North	N. midriff	S. midriff	South
North	0·002 (−0·0107, 0·0147)	0·0005 (0·0001, 0·0015)	1·00	0·62	0·62	−0·21
Northern midriff	−0·027 (−0·0568, 0·0018)	0·0043 (0·0003, 0·0130)	0·62	1·00	0·98	−0·69
Southern midriff	−0·003 (−0·0383, 0·0324)	0·0065 (0·0004, 0·0197)	0·62	0·98	1·00	−0·67
South	0·015 (0·0050, 0·0259)	0·0002 (0, 0·0006)	−0·21	−0·69	−0·67	1·00

Bootstrapped 95% confidence interval for *u* and diagonal elements of **Q** are given in parentheses.

ronmental conditions (ρ = 0·98; Table 2), suggesting that they would be effectively acting as a single subpopulation, were it not for differences in their growth rates and process variances (Table 2; Fig. 2). Across all subpopulations, the process errors have low levels of temporal autocorrelation (acf < 0·2), except for the period 1985–1992, when all but the South subpopulation declined more than expected (acf *c*. 0·5).

Because of missing data, we were forced to restrict our analysis to models with independent observation errors. However, we evaluated support for site-specific observation variances (different values for the variances on the diagonal of **R**) vs. a single level of observation variance across all sites (the same value for the variances on the diagonal of **R**). Our best model supports the latter, with an equal observation variance across all sites (σ^2 = 0·042). Although we were not able to evaluate autocorrelation in observation errors because of missing data, we did find support for the assumption of normal errors using the Shapiro-Wilk test (P = 0·11).

Because the hypotheses about California sea lion population structure were framed independently of our data analysis, even the best model does not fit the data from all sites perfectly (Fig. 2). When comparing the model CI and the data in Fig. 2, note that the CI are for the unknown true subpopulation size, rather than the observations of that size. The 95% CI for the subpopulation sizes should contain less than 95% of the observations because these CI do not account for observation errors. Nonetheless, it is apparent that those sites with the least data have the worst fit (FI in the South subpopulation and RC in the North subpopulation). The model essentially underweights those sites because they have few data points relative to the other sites in the subpopulation with more data. Although we do not advocate data-dredging, in theory it would be possible to construct a MARSS model that would better fit the data by allowing sites with little data to have independent trajectories (for instance FI and LI could be allowed to have opposite trends). The configurations of these sites with sparse data should be re-evaluated after future data is collected.

As expected, the Midriff subpopulations had the highest probabilities of severe declines (50–80%) over the next 50 years (Fig. 3) in our forecasts. Assuming that the negative trend for the Northern Midriff subpopulation continues, there is a > 0·5 probability of the subpopulation experiencing a 50% decline within the next 25 years. In contrast, because of positive growth rates, the North and South subpopulations have low probability of declines > 20% in our projections (Fig. 3). Because the North and South subpopulations appear to be robust and the South subpopulation is acting indepen-

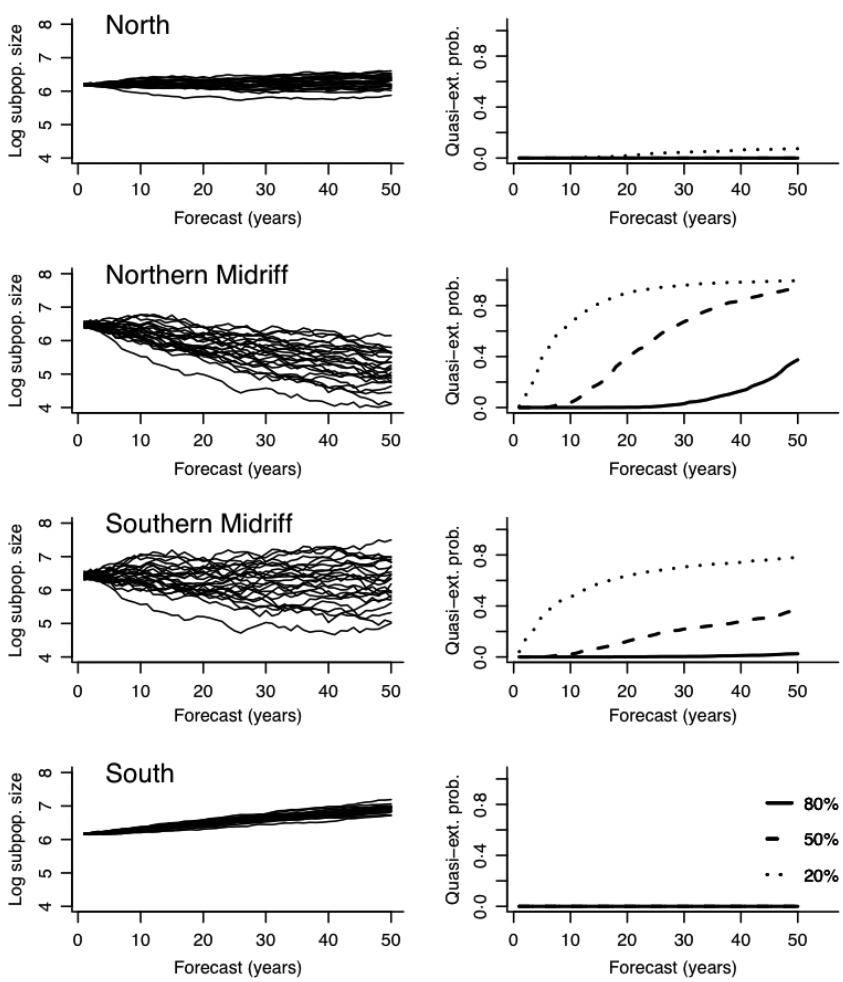

Fig. 3. Risk of 20%, 50% and 80% decline for the four subpopulations defined by the best-fit model. Left panels shows 25 representative trajectories from 1000 subpopulation forecasts. The right panels show the probabilities of 20%, 50% and 80% decline for each of the subpopulations over the next 50 years. The Midriff subpopulations, particularly the Northern Midriff subpopulation, have the highest risks of large declines if past trends continue.

dently of the other subpopulations, our forecasting predicts that California sea lions have little chance of going extinct in the Gulf of California over the next 50 years ($P = 0$ for $>50\%$ declines). However, the centre of abundance would shift south as the South subpopulation contributes an increasing fraction of the total abundance, from 20% in 2006 to 33% in 2030 (and 43% by 2050). Obviously, these forecasts are predicated on the assumption that the past 28 years are a reasonable indication of trends and variability over the next 50 years.

Discussion

A number of ecological analyses have attempted to use biological data to define subpopulations within the California sea lion population in the Gulf of California. The number of estimated subpopulations has varied between two and four, depending on whether subpopulations were assumed to be primarily defined by genetics, diet, disease or geographical distance (Maldonado *et al.* 1995; Szteren 2006; González-Suárez *et al.* 2009; Schramm *et al.* 2009). Each of these analyses has been performed independently, often with different data sources. As a result, comparing the empirical support for these different subpopulation configurations is difficult. In our analysis, we tested each of these previous subpopulation configurations plus two additional configurations, panmictic and 13 independent subpopulations, using a single modelling framework (MARSS), a common data set (multi-site time-series data), and a common scale for measuring data support (likelihood-based model-selection criteria). A MARSS approach does not tell us what biological mechanisms or environmental factors are causing the population structure, but the patterns of synchrony and correlation can help us infer which mechanisms and factors are more important.

We found the population structure with the highest data support has the 13 breeding sites organized into four subpopulations, defined by distance-based clusters, with 2–5 breeding sites in each subpopulation. That multiple, neighbouring, breeding sites are grouped into subpopulations by the MARSS analysis means that the dynamics at these sites are synchronized – they have both the same growth rates and variability and the trajectories do not diverge with time. Dispersal between adjacent sites leads to this type of synchrony because it causes the dynamics across multiple sites to become panmictic. We also found support for a high degree of temporal correlation between the three most northern subpopulations. This means that, while each subpopulation has a unique underlying trajectory and trend, all northern subpopulations appear to have similar temporal deviations in year-to-year growth rates. When one subpopulation experiences a good year, the others are more likely to do so. The strong positive correlation between these subpopulations is probably caused by overlap in environmental conditions and a similar prey base. In contrast, we found a negative correlation between the South subpopulation and all other subpopulations; this may be driven by its geographical remoteness and genetic differences relative to other sites (González-Suárez *et al.* 2009). Further, the environmental variation experienced by the South subpopulation may be affected by its proximity to the Pacific Ocean (Fig. 1).

That we found strong support for subpopulations within the population of California sea lions in the Gulf of California, as opposed to panmictic dynamics, is not surprising. California sea lions have strong fidelity to their natal breeding site and low dispersal rates (Gonzalez-Suarez *et al.* 2006), and the breeding sites in the Gulf of California are spread over a distance that is large relative to the foraging range of this species (800 vs. 40–50 km). The differences in the growth rates across the subpopulations are also not surprising given the large distance between the North and South subpopulation. Analyses of isotopic and scat data suggest that within the Gulf of California population, there are site-level differences in the diet composition and mean trophic level of their prey (Porras-Peters *et al.* 2008). Sea lions from sites in the declining Midriff subpopulations tend to consume prey that is lower on the food chain relative to sea lions in other subpopulations (Porras-Peters *et al.* 2008). This suggests that differences in regional production regimes may be causing some of the differences in growth rates. Sea lions in the Gulf of California also experience anthropogenic disturbances, both directly (entanglement in fishing gear; Zavala-Gonzalez & Mellink 1997) and indirectly (the food web in the Gulf of California being altered by fishing; Sala *et al.* 2004). Although we do not have data on regional differences in these anthropogenic impacts, regional differences in fishing intensity should also be explored as a cause of the regional differences in growth rates. Overall, the North, Midriff and South structure indicates that there are important subpopulation differences and that management efforts based on the overall trends in the Gulf of California may be insufficient at the subpopulation level. Also it indicates that if monitoring funds are limited, monitoring should contain representative samples from each of the four subpopulations.

One of the advantages of using a MARSS modelling framework is that observation error can be explicitly included in the analysis. Ignoring observation error can lead to misleading conclusions about population structure. Independent observation errors cause the abundance counts at different sites to be asynchronous, and suggest, falsely, that their population dynamics are also asynchronous. For instance, if a single subpopulation is observed at multiple sites and there is some degree of asynchrony in observation errors, one can erroneously conclude that the sites represent different independent subpopulations rather than multiple observations of the single subpopulation. Ignoring the observation error would have had serious implications for our analysis of the California sea lions in the Gulf of California. The estimated observation variance for the California sea lion counts was several orders of magnitude larger than the estimated process variance ($\sigma^2 = 0{\cdot}042$ vs. $0{\cdot}004$ and $0{\cdot}0005$). Thus the observed counts at individual breeding sites appear considerably more asynchronous than the true trajectories with observation error removed.

Ignoring observation error also leads to inflated estimates of process variance (the true year-to-year variation driving subpopulation trajectories), and this biases estimates of the risk of decline. The MARSS estimates of process variance are not

inflated because the state-space framework partitions the total variance into process and observation variance (Holmes 2001). However, the lower process variance estimates also mean that estimates of subpopulation viability are less pessimistic than those generated with models that ignore observation error. For example, previous estimates of the probability of 50% declines over 15 years were 0·43 for the Northern Midriff subpopulation (Gonzalez-Suarez *et al*. 2006), compared with our estimate of *c*. 0·20. The MARSS framework also allows us to estimate and model the temporal correlation (positive and negative) between subpopulations. Many studies of extinction risk have shown that accounting for the pattern and level of temporal correlation is critical in metapopulation forecasting (e.g. the recent study by Hinrichsen 2009). In our forecasts of the population as a whole, we found that the risks of decline are low, essentially because of the South subpopulation which is both robust and acting independently of the other subpopulations. Although our forecasts indicate that there is little chance of severe declines at the level of the Gulf of California, our forecasts assume that future conditions will be similar to the last 28 years. Increases in environmental stochasticity, habitat degradation or anthropogenic impacts would translate into greater risks.

At some level, nearly all biological populations are structured spatially (reviews in Bjørnstad, Ims & Lambin 1999 and Hanski 1999). Structure arises naturally because of landscape heterogeneity, barriers to dispersal and geographical isolation which effectively breaks a population into multiple asynchronous subpopulations. Asynchony between subpopulations is one of the most important features allowing metapopulations to persist in the face of local extinctions. At the same time other factors buffer and limit spatial structure and asynchrony. Dispersal dissolves structure by synchronizing what would otherwise be multiple subpopulations into a single panmictic population (Holmes & Semmens 2004). Shared environmental conditions and resource bases correlate subpopulations, limiting their temporal independence from each other. Even across wide geographical distances, population dynamics may become correlated if large-scale environmental conditions are similar enough, a phenomenon known as the 'Moran' effect (e.g. Steinar *et al*. 2005).

It is widely recognized that understanding these patterns of synchrony and correlation are important for conservation and management because these patterns determine whether a metapopulation is able to balance local extinctions and recolonizations (Gilpin 1990; Hanski 1998) and determine how local sites contribute to viability (Goodman 1987). Previous approaches to forecasting metapopulations have assumed that the number of subpopulations is known and that the degree of correlation between subpopulations is known. Yet for many ecological analyses, such as in our analysis of California sea lion population structure, the number of subpopulations is unknown, and in addition, both dispersal rates and the environmental drivers are unknown or poorly monitored. Multivariate state-space models provide a statistical approach for estimating the underlying patterns of synchrony and correlation – and uses only time-series of counts across multiple sites. This provides conservation biologists a new, practical, tool to identify the subpopulations within a metapopulation of concern and to forecast those metapopulations.

Acknowledgements

This study was supported by a grant to LRG from the National Science Foundation (Animal Behavior, Biological Oceanography and International Programs; Award # 0347960), and by funding to DAG provided by CONACyT (Consejo Nacional de Ciencia y Tecnología, grant SEP-2004-C01-46806, and SIP 20070240-20080316). We are grateful to SEMARNAT (Instituto Nacional de Ecología y Dirección de Administración de Pesquerías) for research permits (most recent Oficio num/SGPA/DGVS/03269). Comments from the members of the Gerber lab and two anonymous reviewers considerably improved previous versions of this manuscript. C. D'Agrosa helped create Fig. 1.

References

Aurioles-Gamboa, D. & Zavala-Gonzalez, A. (1994) Algunos factores ecologicos que determinan la distribucion y abundancia del lobo marino *Zalophus californianus*, en el Golfo de California. *Ciencias Marinas*, **20**, 535–553.

Barlow, J. & Forney, K.A. (2007) Abundance and population density of cetaceans in the California current ecosystem. *Fishery Bulletin*, **105**, 509–526.

Bengtsson, T. & Cavanaugh, J.E. (2006) An improved Akaike information criterion for state-space model selection. *Computational Statistics and Data Analysis*, **50**, 2635–2654.

Bjørnstad, O.N., Ims, R.A. & Lambin, X. (1999) Spatial population dynamics: analyzing patterns and processes of population synchrony. *Trends in Ecology and Evolution*, **14**, 427–432.

Bonnell, M.L. & Ford, R.G. (1987) California sea lion distribution: a statistical analysis of aerial transect data. *Journal of Wildlife Management*, **51**, 13–20.

Burnham, K.P. & Anderson, D.R. (2002) *Model Selection and Multimodel Inference*, 2nd edn. Springer Science + Business Media, Inc., New York, NY.

Carretta, J.V., Forney, K.A., Lowry, M., Barlow, J., Baker, J., Hanson, B. & Muto, M.M. (2007) *Draft. U.S. Pacific Marine Mammal Stock Assessments: 2007*. U.S. Department of Commerce, National Oceanic and Atmospheric Administration, La Jolla, CA, pp. 1–9.

Cavanaugh, J.E. & Shumway, R.H. (1997) A bootstrap variant of AIC for state-space model selection. *Statistica Sinica*, **7**, 473–496.

Clark, J.S. & Bjørnstad, O.N. (2004) Population time series: process variability, observation errors, missing values, lags, and hidden states. *Ecology*, **85**, 3140–3150.

Dennis, B., Munholland, P.L. & Scott, J.M. (1991) Estimation of growth and extinction parameters for endangered species. *Ecological Monographs*, **61**, 115–143.

Dennis, B., Ponciano, J.M., Lele, S.R., Taper, M.L. & Staples, D.F. (2006) Estimating density dependence, process noise, and observation error. *Ecological Monographs*, **76**, 323–341.

Garcia-Aguilar, M.C. & Aurioles-Gamboa, D. (2003) Breeding season of the California sea lion (*Zalophus californianus*) in the Gulf of California, Mexico. *Aquatic Mammals*, **29**, 67–76.

Gerber, L.R. (2006) Including behavioral data in demographic models improves estimates of population viability. *Frontiers in Ecology and Environment*, **4**, 419–427.

Gilpin, M.E. (1990) Extinction in finite metapopulations living in correlated environments. *Living in a Patchy Environment* (eds B. Shorrocks & I.R. Swingland), pp. 177–186. Oxford University Press, New York, NY.

Gilpin, M.E. & Hanski, I. (eds) (1991) *Metapopulation Dynamics: Empirical and Theoretical Investigations*. Academic Press, London.

González-Suárez, M. & Gerber, L.R. (2008) A behaviorally-explicit demographic model integrates habitat selection and population dynamics in California sea lions. *Conservation Biology*, **22**, 1608–1618.

Gonzalez-Suarez, M., McCluney, K.E., Aurioles, D. & Gerber, L.R. (2006) Incorporating uncertainty in spatial structure for viability predictions: a case study of California sea lions (*Zalophus californianus californianus*). *Animal Conservation*, **9**, 219–227.

González-Suárez, M., Flatz, R., Aurioles-Gamboa, D., Hedrick, P. & Gerber, L.R. (2009) Isolation by distance among California sea lion populations in Mexico: redefining management stocks. *Molecular Ecology*, **18**, 1088–1099.

Goodman, D. (1987) Considerations of stochastic demography in the design and management of reserves. *Natural Resource Modeling*, **1**, 205–234.

Hanski, I. (1998) Metapopulation dynamics. *Nature*, **396**, 41.

Hanski, I. (1999) *Metapopulation Ecology*. Oxford University Press, Oxford.

Harvey, A.C. (1989) *Forecasting, Structural Time Series Models and the Kalman Filter*. Cambridge University Press, Cambridge.

Hinrichsen, R.A. (2009) Population viability analysis for several populations using multivariate state-space models. *Ecological Modelling*, **220**, 1197–1202.

Hinrichsen, R.A. & Holmes, E.E. (2009) Using multivariate state-space models to study spatial structure and dynamics. *Spatial Ecology* (eds R. Stephen Cantrell, C. Cosner & S. Ruan), pp. 145–166. CRC/Chapman Hall, Boca Raton, FL.

Holmes, E.E. (2001) Estimating risks in declining populations with poor data. *Proceedings of the National Academy of Science*, **98**, 5072–5077.

Holmes, E.E. & Semmens, B.X. (2004) Population viability analysis for metapopulations: a diffusion approximation approach. *Ecology, Genetics, and Evolution of Metapopulations* (eds I. Hanski & O.E. Gaggiotti), pp. 565–598. Elsevier Press, Burlington, MA.

Holmes, E.E., Sabo, J.L., Viscido, S.V. & Fagan, W.F. (2007) A statistical approach to quasi-extinction forecasting. *Ecology Letters*, **10**, 1182–1198.

Jonsen, I.D., Myers, R.A. & Flemming, J.M. (2003) Meta-analysis of animal movement using state space models. *Ecology*, **84**, 3055–3063.

Lele, S.R., Dennis, B. & Lutscher, F. (2007) Data cloning: easy maximum likelihood estimation for complex ecological models using Bayesian Markov chain Monte Carlo methods. *Ecology Letters*, **10**, 551–563.

Levins, R. (1970) Extinction. *Some Mathematical Problems in Biology* (ed. M. Gesternhaber), pp. 77–107. American Mathematical Society, Providence, RI.

Lindley, S.T. (2003) Estimation of population growth and extinction parameters from noisy data. *Ecological Applications*, **13**, 806–813.

Maldonado, J.E., Davila, F.O., Stewart, B.S., Geffen, E. & Wayne, R.K. (1995) Intra-specific genetic differentiation in California sea lions (*Zalophus californianus*) from Southern California and the Gulf of California. *Marine Mammal Science*, **11**, 46–58.

McMahon, C.R., Bradshaw, C.J.A. & Hays, G.C. (2006a) Branding can be justified in vital conservation research. *Nature*, **439**, 392.

McMahon, C.R., Burton, H.R., van den Hoff, J., Woods, R. & Bradshaw, C.J.A. (2006b) Assessing hot-iron and cryo-branding for permanently marking southern elephant seals. *Journal of Wildlife Management*, **70**, 1484–1489.

Mech, L.D. & Shannon, M.B. (2002) *A Critique of Wildlife Radio-Tracking and Its Use in National Parks: A Report to the U.S. National Park Service*. U.S. Geological Survey, Northern Prairie Wildlife Research Center, Jamestown.

Meyer, R. & Millar, R.B. (1999) BUGS in Bayesian stock assessments. *Canadian Journal of Fisheries and Aquatic Sciences*, **56**, 1078–1087.

Newman, K.B., Fernández, C., Thomas, L. & Buckland, S.T. (2009) Monte Carlo inference for state-space models of wild animal populations. *Biometrics*, **65**, 572–583.

Peterson, R.S. & Bartholomew, G.A. (1967) *The Natural History and Behavior of the California Sea Lion*. Special Publication No. 1. The American Society of Mammalogists, Lawrence, KS.

Porras-Peters, H., Aurioles-Gamboa, D., Cruz-Escalona, V.H. & Koch, P.R. (2008) Trophic level and overlap of sea lions (*Zalophus californianus*) in the Gulf of California, Mexico. *Marine Mammal Science*, **24**, 554–576.

Pulliam, H.R. (1988) Sources, sinks, and population regulation. *American Naturalist*, **132**, 652–661.

Roweis, S. & Ghahramani, Z. (1999) A unifying review of linear gaussian models. *Neural Computation*, **11**, 305–345.

Sala, E., Aburto-Oropeza, O., Reza, M., Paredes, G. & López-Lemus, L.G. (2004) Fishing down coastal food webs in the Gulf of California. *Fisheries*, **29**, 19.

Schramm, Y., Mesnick, S.L., de la Rosa, J., Palacios, D.M., Lowry, M.S., Aurioles-Gamboa, D., Snell, H.M. & Escorza-Trevino, S. (2009) Phylogeography of California and Galapagos sea lions and population structure within the California sea lion. *Marine Biology*, **156**, 1375–1387.

Shumway, R.H. & Stoffer, D.S. (2006) *Time Series Analysis and Its Applications*. Springer, New York, NY.

Staples, D.F., Taper, M.L. & Dennis, B. (2004) Estimating population trend and process variation for PVA in the presence of sampling error. *Ecology*, **85**, 923–929.

Steinar, E., Lande, R., Saether, B.E. & Bregnballe, T. (2005) Estimating the pattern of synchrony in fluctuating populations. *Journal of Animal Ecology*, **74**, 601–611.

Stoffer, D.S. & Wall, K.D. (1991) Bootstrapping state-space models: Gaussian maximum-likelihood estimation and the Kalman filter. *Journal of the American Statistical Association*, **86**, 1024–1033.

Szteren, D. (2006) *Regionalizacion ecologica de las colonias reproductivas de Zalophus c. californianus en el Golfo de California, Mexico*, PhD Dissertation. CICIMAR – Instituto Politecnico Nacional, La Paz, Baja California Sur, Mexico, 180p.

Szteren, D., Aurioles, D. & Gerber, L.R. (eds) (2006) *Population Status and Trends of the California Sea Lion (Zalophus californianus californianus) in the Gulf of California, Mexico, Vol. Alaska Sea Grant College Program*. University of Alaska Fairbanks, Fairbanks, AK.

Tilman, D. & Kareiva, P. (1997) *Spatial Ecology: The Role of Space in Population Dynamics and Interspecific Interactions*. Princeton University Press, Princeton.

de Valpine, P. & Hastings, A. (2002) Fitting population models incorporating process noise and observation error. *Ecological Monographs*, **72**, 57–76.

Ward, E.J., Hilborn, R., Towell, R.G. & Gerber, L. (2007) A state-space mixture approach for estimating catastrophic events in time series data. *Canadian Journal of Fisheries and Aquatic Sciences*, **644**, 899–910.

Wielgus, J., Gonzalez-Suarez, M., Aurioles-Gamboa, D. & Gerber, L.R. (2008) A noninvasive demographic assessment of sea lions based on stage-specific abundances. *Ecological Applications*, **18**, 1287–1296.

Zavala-Gonzalez, A. & Mellink, E. (1997) Entanglement of California sea lions, *Zalophus californianus californianus* in fishing gear in the central-northern part of the Gulf of California, Mexico. *Fishery Bulletin*, **95**, 180–184.

Zavala-Gonzalez, A. & Mellink, E. (2000) Historical exploitation of the California sea lion, *Zalophus californianus*, in Mexico. *Marine Fisheries Review*, **62**, 35–40.

Received 23 July 2009; accepted 17 November 2009
Handling Editor: Chris Wilcox